ACCSCIENCE PUBLISHING

Eurasian Journal of Medicine and Oncology

ORIGINAL RESEARCH ARTICLE

Chemical characterization and hypothesis generating network pharmacology analysis of Shenfu Qiangxin pill

Haiyun Zhu[1]* and Yingdong Wu[2]

[1]Department of Cardiology, Tianjin Academy of Traditional Chinese Medicine Affiliated Hospital, Tianjin, China

[2]Graduate School, Tianjin University of Traditional Chinese Medicine, Tianjin, China

Abstract

Introduction: Heart failure represents a heavy global clinical medical burden with unsatisfactory long term outcomes under conventional therapeutic regimens. Traditional Chinese medicine exerts beneficial effects for chronic heart failure management via multi-component and multi-target modes of action. Shenfu Qiangxin pill (SFQXP) is a clinically effective herbal formula for chronic heart failure treatment, yet its systematic chemical profiling and underlying molecular mechanisms remain poorly characterized.

Objective: To characterize the chemical constituents of SFQXP and generate testable hypotheses for heart failure-relevant mechanisms using ultra-high-performance liquid chromatography quadrupole orbitrap high-resolution mass spectrometry (UHPLC-Q-Orbitrap-HRMS), network pharmacology, and molecular docking.

Methods: *In vitro* extracts and rat medicated serum were analyzed using UHPLC Q Orbitrap HRMS. Constituents were tentatively annotated against TCM Pro 2.0 and an in-house compound library. Active compounds were screened via SwissADME. Drug related and heart failure associated targets were retrieved from SwissTargetPrediction, GeneCards, and OMIM. Intersection targets were subjected to protein–protein interaction network construction, core target filtering, and Gene Ontology/Kyoto Encyclopedia of Genes and Genomes enrichment analyses. AutoDock Vina 1.1.2 was used to evaluate molecular docking between sanggenol A and peroxisome proliferator-activated receptor gamma (PPARG).

Results: A total of 232 non redundant constituents (186 *in vitro*, 151 serum derived; 105 shared) were annotated at MSI Level 2 without authentic reference standards. Thirty five bioactive candidates and 125 overlapping drug disease targets were obtained, and 33 core targets were screened. Enrichment analyses highlighted cyclic guanosine monophosphate protein kinase G, cyclic adenosine monophosphate, and calcium signaling pathways associated with ventricular remodeling. Sanggenol A exhibited favorable *in silico* predicted binding affinity (−8.3 kcal/mol) to PPARG.

Conclusion: This study profiles SFQXP chemical components and puts forward computational mechanistic hypotheses. Anti heart failure bioactivity has not been experimentally validated; further cellular and animal model experiments are required for verification.

Keywords: Shenfu Qiangxin Pill; Heart failure; Ultra-high-performance liquid chromatography quadrupole orbitrap high-resolution mass spectrometry; Network pharmacology; Molecular docking; Ventricular remodeling

***Corresponding author:**
Haiyun Zhu
(zhuhaiyuns@126.com)

Citation: Zhu H, Wu Y. Chemical characterization and hypothesis generating network pharmacology analysis of Shenfu Qiangxin pill. *Eurasian J Med Oncol.* doi: 10.36922/EJMO026370506

Received: September 13, 2026

Revised: October 24, 2026

Accepted: October 26, 2026

Published online: November 19, 2026

Copyright: © 2026 Author(s). This is an Open-Access article distributed under the terms of the Creative Commons Attribution License, permitting distribution, and reproduction in any medium, provided the original work is properly cited.

Publisher's Note: AccScience Publishing remains neutral with regard to jurisdictional claims in published maps and institutional affiliations.

1. Introduction

Heart failure (HF) represents a severe clinical syndrome triggered by cardiac structural and functional abnormalities that impair ventricular systolic or diastolic performance. High morbidity, readmission rates, and mortality of HF create substantial global medical care burdens.[1] Although conventional pharmacological interventions, including diuretics, angiotensin-converting enzyme inhibitors/ angiotensinreceptor blockers, and βblockers, improve clinical outcomes, adverse events and unsatisfactory longterm therapeutic efficacy remain unresolved clinical challenges.[1,2]

Traditional Chinese medicine (TCM) exhibits unique advantages for preventing and managing chronic HF through holistic modulation and multitarget pharmacological characteristics. Shenfu Qiangxin pill (SFQXP) is a modified herbal preparation derived from Jijiao Lihuang pill and Shenfu decoction, formulated by Professor Ma Lianzhen according to the TCM pathogenesis pattern defined as "heart–kidney yang deficiency, blood stasis, and water retention".[3] Its herbal composition includes Ginseng radix et rhizoma, Aconiti lateralis radix praeparata, Lepidii semen, Rhei radix et rhizoma, Mori cortex, and Polyporus. Prior clinical investigations confirm that SFQXP can markedly improve cardiac function and relieve clinical symptoms in patients with chronic HF, with an acceptable safety profile.[4-8] Nevertheless, systematic chemical profiling and the precise molecular mechanism of SFQXP remain largely unelucidated, hindering its modern research and international popularization.

Ultra-highperformance liquid chromatographhybrid quadrupole orbitrap highresolution mass spectrometer (UHPLCQOrbitrap HRMS) permits rapid, sensitive, and accurate identification of complex chemical components within TCM compound formulas.[9] Network pharmacology provides a systematic analytical workflow for deciphering "drugcomponenttargetsignaling pathway" regulatory networks.[10] In this work, we integrated UHPLCQOrbitrap HRMS, network pharmacology, and molecular docking to characterize the chemical constituents of SFQXP, screen bioactive ingredients, predict core therapeutic targets and downstream signaling cascades, and verify key molecular interactions. This study aims to explore the potential pharmacodynamic basis of SFQXP and generate computational hypotheses about HF-relevant molecular mechanisms.

2. Materials and methods

2.1. Materials

Shenfu Qiangxin pill was obtained from Darentang Pharmaceutical Co., Ltd. (China). Liquid chromatography-mass spectrometrygrade methanol, acetonitrile, and formic acid were purchased from ThermoFisher Scientific (United States). Ultrapure water was generated with a MilliQ waterpurification instrument (Millipore, United States).

2.2. Animals

Male specificpathogenfree SpragueDawley rats (n = 20; 6 weeks old; body weight 180–220 g) were supplied by Sibeifu Biotechnology Co., Ltd. (China). All animal experimental protocols received ethical approval from the Experimental Animal Ethics Committee (approval No. IACUCGENINK20250160). Animal handling and operations strictly complied with the Guide for the Care and Use of Laboratory Animals.

2.3. Sample preparation

2.3.1. In vitro extract

A total of 1.0 g SFQXP powder was extracted with 40 mL of 80% methanol under ultrasonic treatment (250 W, 40 kHz) for 30 mins. After centrifugation at 12,000 rpm for 10 mins at 4 °C, the resulting supernatant was filtered via a 0.22 μm microporous membrane for instrumental analysis.

2.3.2. Rat-medicated serum

Rats were randomly allocated to four experimental groups (n = 5): control group, SFQXP lowdose group, SFQXP mediumdose group, and SFQXP highdose group. The dosages were converted according to body surface area normalization for human–rat equivalence. The medium dose (3.6 g/kg) was converted from the clinical human daily dose of SFQXP; the low dose (1.8 g/kg) and high dose (7.2 g/kg) were set at 0.5fold and 2fold of the medium dose, respectively. Random group assignment was implemented using simple random sampling. The control group received an equal volume of 0.9% sodium chloride normal saline vehicle. Animals received intragastric drug administration for three consecutive days. Blood specimens were collected at 0, 30, 60, 90, and 120 mins following the final intragastric gavage. Serum fractions were separated and stored at −80 °C. Serum samples from rats within the same group and time point were pooled before deproteinization and UHPLC-Q-Orbitrap HRMS measurement, rather than analyzing individual rat samples. A sample size of n = 5 per group follows conventional practice for rat serum pharmacochemistry studies. Blinding was not implemented for drug administration and sample preparation procedures in this work. Serum samples were deproteinized with methanol, filtered, and analyzed by UHPLC-Q-Orbitrap HRMS.

2.4. Ultra-high-performance liquid chromatograph hybrid quadrupole orbitrap high-resolution mass spectrometer conditions

2.4.1. Chromatographic conditions

Chromatographic separation was performed on an ACQUITY UPLC HSS T3 analytical column (2.1 mm × 100 mm, 1.8 μm; Waters Corporation, United States). Mobile phase A was an aqueous solution containing 0.1% formic acid; mobile phase B was pure acetonitrile. Gradientelution procedures were applied. The flow rate was set to 0.3 mL/min, the column temperature to 40 °C, and the injection volume to 6.0 μL (Table 1).

Table 1. Gradientelution program for ultra-high-performance liquid chromatography separation

Time (min)	Mobile phase	
	A (v%)	B (v%)
0	98	2
1.0	98	2
14.0	70	30
25.0	0	100
28.0	0	100
28.1	98	2
30.0	98	2

2.4.2. Mass spectrometry conditions

A Q Exactive™ HRMS (ThermoFisher Scientific, United States) equipped with an electrospray ionization source was operated under positiveion and negativeion acquisition modes. The parameters were: spray voltage: 3.7 kV (positive mode), 3.5 kV (negative mode); capillary temperature: 320 °C; sheathgas flow: 30 arb; auxiliarygas flow: 10 arb; heater temperature: 300 °C. Raw mass spectrometry signals were acquired in full-scan /datadependent MS^2 ($ddMS^2$) mode. Fullscan parameters were: resolution: 70,000 FWHM; automatic gain control setting: 1×10^6 ions; and masstocharge ratio (m/z) scan window: 100–1,500. $ddMS^2$ fragmentation parameters were: resolution: 17,500 FWHM; automatic gain control setting: 1×10^5 ions; and stepped normalized collision energy: 10, 30, 60 eV.

2.5. Data processing

Original mass spectrometric raw datasets were processed using Progenesis QI 3.0 software. Chemical constituents were identified by matching experimental accurate mass values, isotope patterns, and tandem mass spectrometry fragment spectra against the TCM Pro 2.0 database and an inhouse theoretical compound library. A total of 186 constituents were identified from *in vitro* extracts, and 151 constituents were characterized in rat-medicated serum.

All detected chemical constituents in this work were tentatively annotated based on matching accurate mass, isotope patterns, and tandem mass spectrometry fragmentation spectra against the TCM Pro 2.0 database and an inhouse theoretical compound library. No authentic reference standards were used for definitive confirmation. The mass error cutoff for candidate annotation was set within ±5 ppm. Compound identification confidence was assigned at level 2 (putative annotation according to MSI metabolomics standard: tentative identification by mass spectrometry without reference standard). Isomeric compounds could not be comprehensively distinguished under current analytical conditions. The total number of unique constituents (232) was calculated as follows: 186 *in vitro*-derived compounds + 151 serumdetected compounds − 105 overlapping shared compounds = 232 nonredundant constituents.

Notably, none of the annotated constituents, including the key compound sanggenol A, were confirmed using authentic reference standards. All compounds, including sanggenoltype flavonoids, are assigned to MSI Level 2 tentative identification based solely on mass spectrometric database matching.

2.6. Network pharmacology analysis

2.6.1. Active component screening

Candidate bioactive compounds were screened USING SwissADME according to Lipinski's Rule of Five, Veber's rules, and PAINS filter criteria. Compounds with favorable gastrointestinal absorption and fulfilling ≥ 2 druglikeness criteria were retained. After screening, 35 potential active ingredients were obtained (Table 2). These cutoffs represent common preliminary filtering for orally absorbed smallmolecule candidates in traditional medicine computational studies.

2.6.2. Target prediction

Compoundderived putative targets were predicted with SwissTargetPrediction; entries with prediction probability = 0 were discarded, followed by deduplication, yielding 196 compoundrelated targets. HFassociated disease targets were retrieved from GeneCards (version 5.16) (relevance score > 5), converted to *Rattus norvegicus* orthologous genes and deduplicated, resulting in 4,281 diseaserelated genes. The OMIM database was also queried but yielded a relatively small gene set.

Table 2. Information on 35 candidate bioactive compounds from Shenfu Qiangxin pill

No.	Name	SMILES format	Source
1	2-methyl-5-carboxymethyl-7-hydroxychromone	Cc1cc(=O)c2c(CC(=O)O)cc(O)cc2o1	1
2	7-hydroxy-2-(2-hydroxy)propyl-5-methyl-benzopyran -gamma-one	Cc1cc(O)cc2oc(CC(C)O)cc(=O)c12	1
3	Cassiachromone	CC(=O)Cc1cc(O)cc2oc(C)cc(=O)c12	1
4	Magnolol	C=CCC1=CC(=C(C=C1)O)C2=C(C=CC(=C2)CC=C)O	2
5	Perlolyrine	C1=CC=C2C(=C1)C3=C(N2)C(=NC=C3)C4=CC=C(O4)CO	2
6	6-demethyldesoline	CCN1C[C@]2(COC)CC[C@H](O)[C@]34[C@H]1[C@](O)([C@@H](O)[C@H]23)[C@@]1(O)C[C@@H](OC)[C@H]2C[C@@H]4[C@@H]1[C@H]2OC	3
7	Atisine	C=C1[C@H]2CC[C@@]3(CC[C@H]4[C@@]5(CCC[C@@]4(C)CN4CCO[C@H]45)[C@@H]3C2)[C@@H]1O	3
8	Bullatine b	CCN1CC2(COC)CCC(O)C34C5CC6C(OC)CC(O)(C5C6O)C(C(OC)C23)C14	3
9	Bullatine g	CCN1C[C@@]2(CC[C@@H]([C@@]34[C@@H]2C[C@@H]([C@H]31)[C@]56[C@H]4CC(=O)[C@H](C5)C(=C)[C@H]6O)O)C	3
10	Carmichaeline	CCN1CC2(C)CCC(O)C34C5CC6C(OC)CC(O)(C(CC23)C14)C5C6O	3
11	Chasmanine	CCN1CC2(COC)CCC(OC)C34C5CC6C(OC)CC(O)(C5C6O)C(C(OC)C23)C14	3
12	Dictysine	CN1CC2(C)CCCC34C1C(CC23)C12CCC(CC41)C(O)(CO)C2O	3
13	Fuziline	CCN1CC2(CCC(C34C2C(C(C31)C5(C6C4CC(C6O)C(C5O)OC)O)OC)O)COC	3
14	Hetisine	C=C1CC23CC4C5C6(C)CC(O)CC57C(C2C(O)C1C(O)C37)N4C6	3
15	Hypaconine	CN1CC2(CCC(C34C2C(C(C31)C5(C6C4CC(C6O)(C(C5O)OC)O)O)OC)OC)COC	3
16	Napelline	C=C1C2CC3(C1O)C1CC4C5(C)CCC(O)C4(C1N(CC)C5)C3CC2O	3
17	Senbusine A	CCN1CC2(COC)CCC(O)C34C5CC6C(OC)CC(O)(C5C6O)C(C(O)C23)C14	3
18	Talatisamine	CCN1CC2(CCC(C34C2CC(C31)C5(CC(C6CC4C5C6O)OC)O)OC)COC	3
19	2,4,2',4'-tetrahydroxy -3'-prenylchalcone	CC(C)=CCc1c(O)ccc(C(=O)C=Cc2ccc(O)cc2O)c1O	4
20	Aromadendrin	O=C1c2c(O)cc(O)cc2OC(c2ccc(O)cc2)C1O	4
21	Cyclocommunol	CC(C)=CC1Oc2cc(O)ccc2-c2oc3cc(O)cc(O)c3c(=O)c21	4
22	Eudraflavone B hydroperoxide	CC1(C)C=Cc2c(cc(O)c3c(=O)c4c(oc23)-c2ccc(O)cc2O[C@H](C(C)(C)OO)C4)O1	4
23	Kuwanon S	CC(C)=CCC/C(C)=C/Cc1cc(-c2cc(=O)c3c(O)cc(O)cc3o2)ccc1O	4
24	Kuwanon U	COc1cc(O)c(C2CC(=O)c3c(O)cc(O)cc3O2)cc1C/C=C(\C)CCC=C(C)C	4
25	Moracin P	CC1(C)Oc2cc3oc(-c4cc(O)cc(O)c4)cc3cc2CC1O	4
26	Morusignin L	CC(C)(O)CCc1c(-c2ccc(O)cc2O)oc2cc3c(c(O)c2c1=O)C=CC(C)(C)O3	4

(*Cont'd...*)

Table 2. (*Continued*)

No.	Name	SMILES format	Source
27	Morusin	CC(=CCC1=C(OC2=C(C1=O)C(=CC3=C2C=CC(O3)(C)C)O)C4=C(C=C(C=C4)O)O)C	4
28	Naringenin	C1[C@H](OC2=CC(=CC(=C2C1=O)O)O)C3=CC=C(C=C3)O	4
29	Neocyclomorusin	CC1(C)C=Cc2c(cc(O)c3c(=O)c4c(oc23)-c2ccc(O)cc2OC(C(C)(C)O)C4)O1	4
30	Sanggenol A	CC(C)=CCC/C(C)=C/Cc1c(O)ccc([C@@H]2CC(=O)c3c(O)cc(O)cc3O2)c1O	4
31	Sanggenol L	CC(C)=CCCC1(C)C=Cc2c(cc(O)c3c2OC(c2ccc(O)cc2O)CC3=O)O1	4
32	Sanggenon M	CC(C)=CC[C@]12Oc3c4c(cc(O)c3C(=O)[C@@]1(O)Oc1cc(O)ccc12)OC(C)(C)C=C4	4
33	Sanggenone I	CC(C)=CCC[C@]1(C)C=Cc2c(O)ccc([C@H]3CC(=O)c4c(O)cc(O)cc4O3)c2O1	4
34	Scopolin	COC1=C(C=C2C(=C1)C=CC(=O)O2)O[C@H]3[C@@H]([C@H]([C@@H]([C@H](O3)CO)O)O)O	4
35	Skimmin	C1=CC(=CC2=C1C=CC(=O)O2)O[C@H]3[C@@H]([C@H]([C@@H]([C@H](O3)CO)O)O)O	4

Note: Source: 1 = Rhei radix et rhizoma; 2 = Compound herbal formula; 3 = Aconiti lateralis radix praeparata; 4 = Mori cortex.

Subsequent analysis adopted intersecting genes between compoundderived targets and GeneCards disease genes, and 125 overlapping target genes were acquired for downstream analyses. Targets with probability = 0 were removed to filter extremely lowconfidence predictions; a GeneCards relevance score > 5 was applied to exclude weakly associated background disease genes. The OMIM database retrieved only a very limited number of HF-related entries, and GeneCards (relevance score > 5) was the predominant source of diseaseassociated genes. This filtering setting may introduce potential selection bias for downstream intersection target and enrichment analyses. The relevance score >5 cutoff was applied to exclude weakly associated lowconfidence background gene entries.

2.6.3. Protein–protein interaction network construction and coretarget screening

Overlapping target genes were uploaded to the STRING database (confidence score ≥ 0.7). The resulting protein–protein interaction (PPI) network was visualized using Cytoscape 3.9.1. Three topological parameters, including degree centrality, closeness centrality, and betweenness centrality, were calculated. Candidate core targets were preliminarily obtained from topological indices, and the final core targets were determined after secondary screening. STRING (version 12.0) confidence score ≥0.7 was chosen to retain only highconfidence PPI pairs.

2.6.4. Gene Ontology and Kyoto Encyclopedia of Genes and Genomes enrichment analysis

Gene Ontology (GO) and Kyoto Encyclopedia of Genes and Genomes (KEGG)[11] enrichment analyses were performed using the clusterProfiler package in R (version 4.4.4). Enrichment terms with $p < 0.05$ were regarded as statistically significant.

The Benjamini–Hochberg false discovery rate correction was applied for multiple-testing adjustment; terms with adjusted $p < 0.05$ were considered statistically significant for GO and KEGG enrichment.

2.6.5. Molecular docking

Among multiple core targets from the PPI network, peroxisome proliferator-activated receptor gamma (PPARG) was selected as the representative receptor for case study molecular docking, given its established role in regulating myocardial fibrosis and inflammatory responses closely linked to HF progression. Sanggenoltype flavonoids (sanggenol A, sanggenol L, sanggenol I, sanggenon M) are serumdetected characteristic bioactive compounds from

the Mori cortex of SFQXP and received high prediction probabilities for PPARG from SwissTargetPrediction. These four compounds were chosen as representative ligands for docking simulation (not exhaustive docking for all core targets). Among these four serumdetected sanggenoltype flavonoids, sanggenol A was selected as the primary docking ligand because it had the highest target-prediction probability for PPARG in the SwissTargetPrediction results. All docking affinity results are purely computational simulation outputs and do not represent experimental proof of physical binding or cellular bioactivity.

Molecular docking is a computational method for predicting the preferred binding orientation of a smallmolecule ligand to a receptor macromolecule such as protein, RNA, or enzyme. In this study, semiflexible docking was performed to generate stable ligand–receptor complexes. This approach is essential for deciphering molecular mechanisms and screening lead compounds, and it is a fundamental technique for structurebased drug design.

Sanggenol A (the topranked active compound predicted by SwissTargetPrediction) was docked against PPARG (UniProt ID: O88275) using AutoDock Vina 1.1.2.[12] Combined strategies integrating multiple docking packages and machine learning algorithms can further improve prediction performance for network pharmacology research.[13] The twodimensional compound structure was retrieved from the PubChem database. Its threedimensional conformation was constructed and energyminimized using ChemDraw 20.0. The PPARG protein structural model was downloaded from the AlphaFold Protein Structure Database (https://alphafold.ebi.ac.uk/). Protein preprocessing, including removal of modelled water artefacts and addition of hydrogen atoms, was carried out in PyMOL 2.4. AutoDock Tools 1.5.6 was applied to generate PDBQT input files for docking simulation. The docking box center coordinates were set to (14.6 Å, 26.1 Å, −9.4 Å), with dimensions of 70 Å × 70 Å × 70 Å, to fully enclose the whole receptor protein, while other parameters were kept at default values. A total of 20 docking poses were output. The pose with the lowest binding energy was considered the most favorable predicted binding mode between the ligand and receptor. AutoDock Vina outputs relative root-mean-square deviation (RMSD) values comparing alternative docking poses against the lowestenergy pose; no absolute RMSD value was generated for the lowestenergy pose itself. After screening 20 generated poses, the pose with the most favorable binding affinity (−8.3 kcal/mol) was selected as the optimal binding conformation for subsequent interaction analysis. Final docking poses were visualized in PyMOL 2.4 and Discovery Studio 2019 to show ligand–receptor interactions and assess complex stability. Dockingresult evaluation criteria: Lower binding energy indicates stronger binding affinity. Ligands exhibit marginal binding activity when binding energy < −4.25 kcal/mol, satisfactory binding activity at < −5.0 kcal/mol, and tight binding activity at < −7.0 kcal/mol.[12]

It should be noted that the PPARG threedimensional structure used herein was retrieved from the AlphaFold protein structure database rather than an experimentally resolved crystallographic PDB entry. A semiblind docking strategy with a fullprotein docking box was adopted to explore potential binding pockets across the whole receptor. No crystallographic redocking validation was performed for this artificial intelligence-predicted protein model, which cannot eliminate structural uncertainties originating from AlphaFoldpredicted protein structures. Future docking analyses using experimentally determined PDB structures together with a confined activesite docking box will improve the reliability of ligand–receptor interaction prediction.

3. Results

3.1. Identification of chemical constituents

In total, 186 chemical constituents were detected in the *in vitro* herbal extract, and 151 compounds were detected in rat-treated serum (Figure 1). Major compound categories included prenyl lipids (from Aconiti lateralis radix praeparata and Ginseng radix et rhizoma), flavonoids (from Mori cortex), and anthracenes (from Rhei radix et rhizoma). A total of 35 candidate bioactive components were screened. A total of 232 non-redundant characterized constituents were identified.

3.2. Component–target–disease network

Altogether, 196 componentderived targets and 4,281 HFassociated disease targets were retrieved, yielding 125 overlapping target genes. The constructed "herb–component–target" network contained 164 nodes and 448 edges (Figure 2).

3.3. Protein–protein interaction network and coretarget identification

The PPI network (STRING confidence score ≥ 0.7) was imported into Cytoscape for topologicalparameter calculation (Figure 3). Three topological parameters, including degree centrality, closeness centrality, and betweenness centrality, were calculated. Candidate core targets were preliminarily obtained from topological indices (Figure 3C), and the final core targets were determined after secondary screening (Figure 3D), including PPARG,

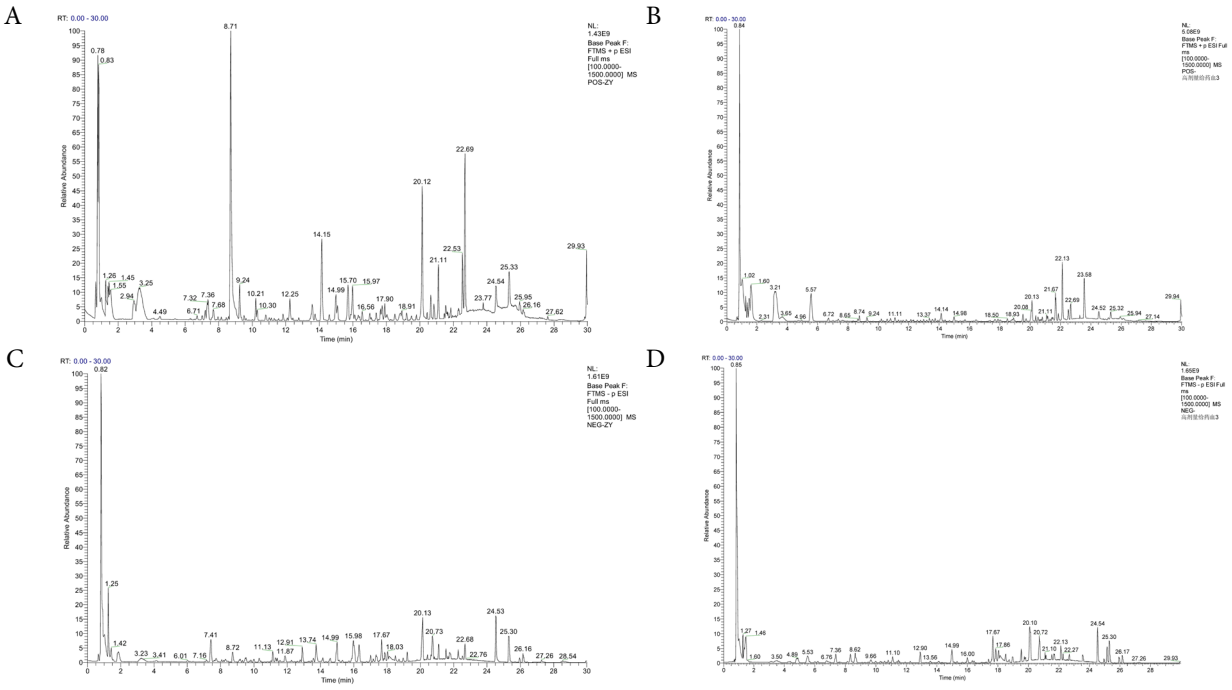


Figure 1. Base-peak chromatograms (BPC) of Shenfu Qiangxin pill (SFQXP) samples detected by ultra-high-performance liquid chromatography quadrupole orbitrap high-resolution mass spectrometry. Representative BPCs obtained under positive-ion mode for (A) SFQXP *in vitro* extract and (B) rat-medicated serum; under negative-ion mode for (C) SFQXP *in vitro* extract and (D) rat-medicated serum. Chromatographic separation was performed on an ACQUITY UPLC HSS T3 column with the gradient elution program described in Table 1.

protein kinase 1, tumor necrosis factor, and interleukin-6.

3.4. Gene Ontology and Kyoto Encyclopedia of Genes and Genomes enrichment analysis

Gene Ontology enrichment analysis identified multiple enriched terms across biological process, cellular component, and molecular function. KEGG analysis identified 38 statistically significant enriched signaling pathways, including neuroactive ligand–receptor interaction, cyclic guanosine monophosphateprotein kinase G (cGMPPKG), cyclic adenosine monophosphate (cAMP) signaling pathway, and calcium signaling pathway (Figure 4).[11,14]

3.5. Molecular docking validation

A total of 20 docking poses were generated by AutoDock Vina for sanggenol A and PPARG (Figure 5). Among all generated poses, the optimal conformation showed the highest binding affinity of −8.3 kcal/mol. Relative RMSD metrics were calculated between each alternative pose and this optimal pose, and no absolute RMSD value was assigned to the optimal pose itself. In this energetically favorable conformation predicted by semi-blind docking, sanggenol A inserts deep into a putative PPARG ligand-binding pocket, forming stable hydrogen-bond interactions with Ser289 and His323, along with multiple hydrophobic contacts with surrounding pocket residues, indicating a computationally predicted stable ligand–receptor complex. Notably, these docking outputs are purely computational predictions and do not constitute experimental evidence for physical proteinligand interaction or biological function. Docking simulation results for three additional sanggenol-type flavonoids (sanggenol L, sanggenol I, sanggenon M) against PPARG are summarized in Table 3, and their two-dimensional and three-dimensional ligand–receptor interaction diagrams are presented in Figure 6.

4. Discussion

This study characterized the chemical composition profile of SFQXP by UHPLCQOrbitrap HRMS and identified potential HFrelevant pharmacological mechanisms by combining network pharmacology prediction and molecular docking verification. A total of 186 *in vitro* and 151 serumderived constituents were identified; 35 potential bioactive compounds and 125 intersecting drug–disease targets were obtained, reflecting the inherent multicomponent and multitarget therapeutic characteristics of this TCM formula.

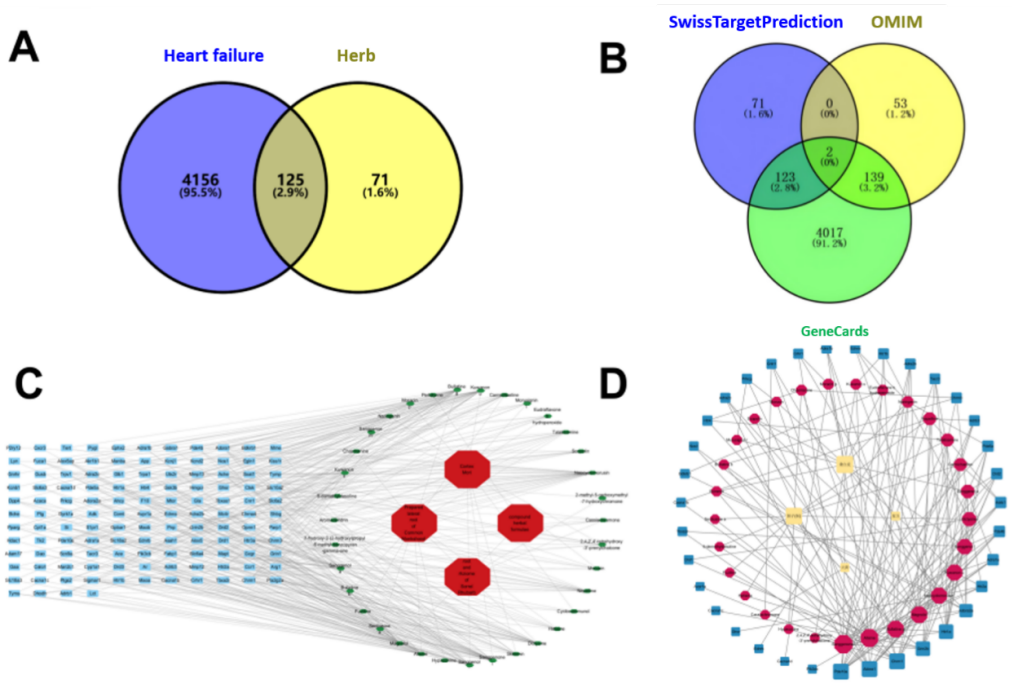


Figure 2. Target screening and intersection analysis between Shenfu Qiangxin pill-related targets and heart failure-associated genes based on *in silico* computational analysis. (A) Venn diagram showing overlapping targets of Shenfu Qiangxin pill putative targets and heart failure-related genes retrieved from the GeneCards database (relevance score > 5). (B) Venn diagram integrating target datasets from SwissTargetPrediction, GeneCards, and OMIM databases. (C) Compound–target–disease interaction network constructed using Cytoscape 3.9.1. (D) Visualization of the intersection target dataset.
Note: All analyses are computational predictions without in vitro/in vivo functional statistical validation.

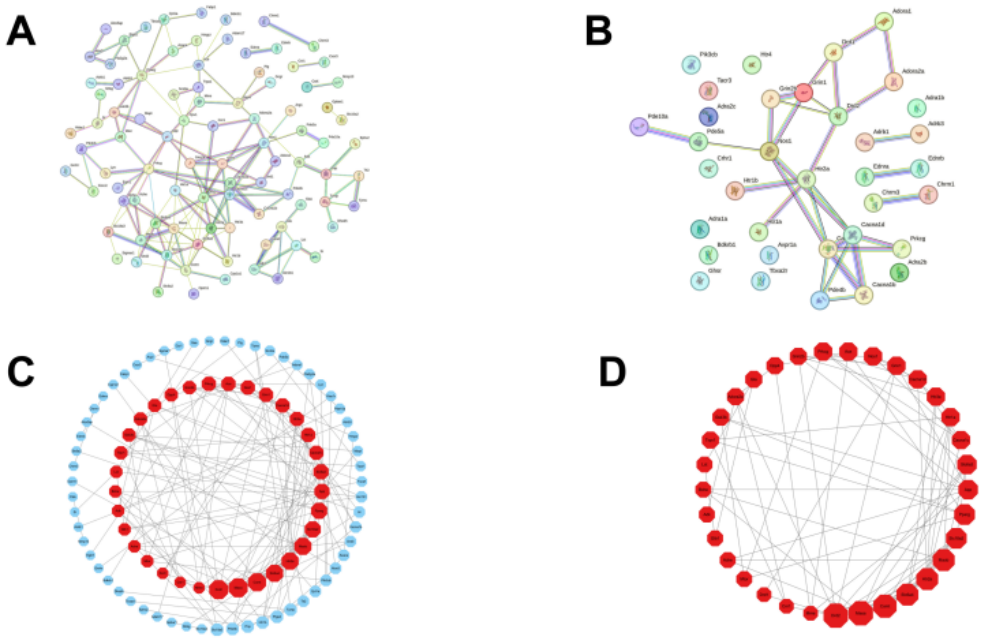


Figure 3. Protein–protein interaction (PPI) networks of intersecting targets between Shenfu Qiangxin pill and heart failure. (A) PPI network built in the STRING database with interaction confidence score ≥0.4 (presented for preliminary visual overview only and not used for downstream calculation). (B) PPI network filtered with confidence score ≥0.7; this highconfidence dataset was used for all subsequent topological calculations and coretarget screening. (C) Preliminary coretarget network filtered by three topological indices (degree centrality, closeness centrality, betweenness centrality). (D) Final coretarget network after secondary topological screening in Cytoscape 3.9.1.

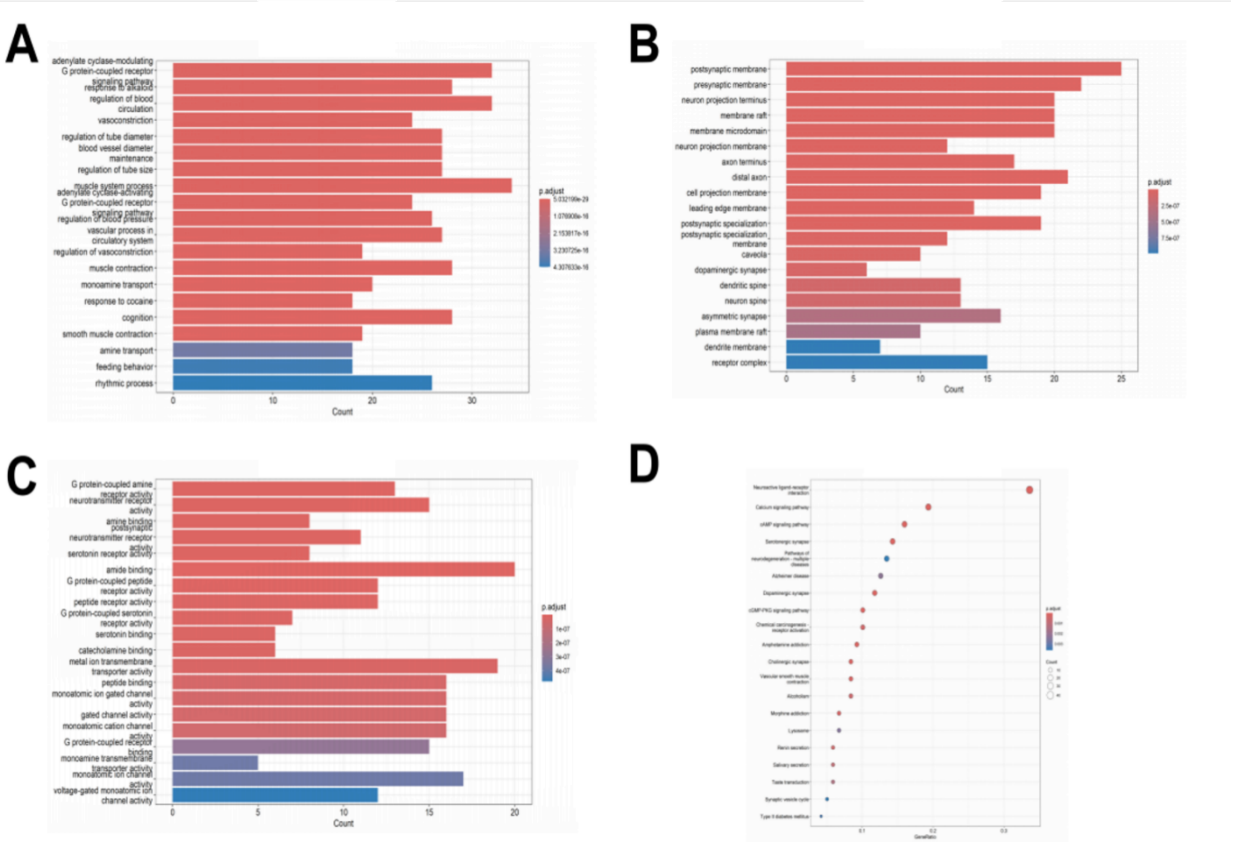


Figure 4. Gene Ontology and Kyoto Encyclopedia of Genes and Genomes enrichment analyses for the 125 overlapping target genes (cutoff threshold: adjusted $p < 0.05$ after Benjamini–Hochberg multipletesting correction). (A) Top enriched Gene Ontology biological process terms. (B) Top enriched Gene Ontology cellular component terms. (C) Top enriched Gene Ontology molecular function terms. (D) Bubble plot visualization of significantly enriched Kyoto Encyclopedia of Genes and Genomes signaling pathways. Enrichment calculations were performed using the clusterProfiler package in R.

Table 3. Summary of moleculardocking affinity values of sanggenoltype flavonoids against peroxisome proliferator-activated receptor gamma

Compound	Binding affinity (kcal/mol)
Sanggenol A	−8.3
Sanggenol L	−7.9
Sanggenol I	−7.7
Sanggenon M	−8.1

Note: Binding affinity values correspond to the optimal docking pose of each compound. These are *in silico* simulation results and are not experimentally measured binding data.

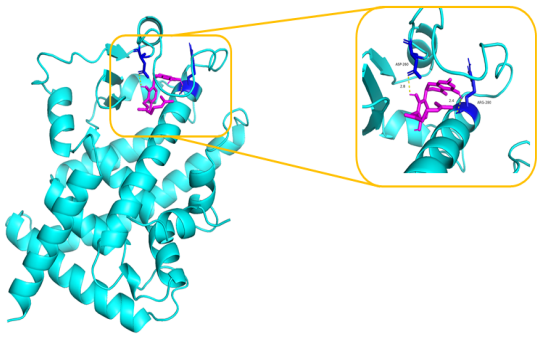


Figure 5. Molecular docking simulation of sanggenol A binding to peroxisome proliferator-activated receptor gamma protein (*in silico* analysis using AutoDock Vina 1.1.2). Overall three-dimensional docking conformation (left); magnified local view of ligandreceptor binding pocket (middle); two-dimensional interaction diagram displaying hydrogen-bond and hydrophobic contacts (right). Optimal binding affinity = −8.3 kcal/mol.

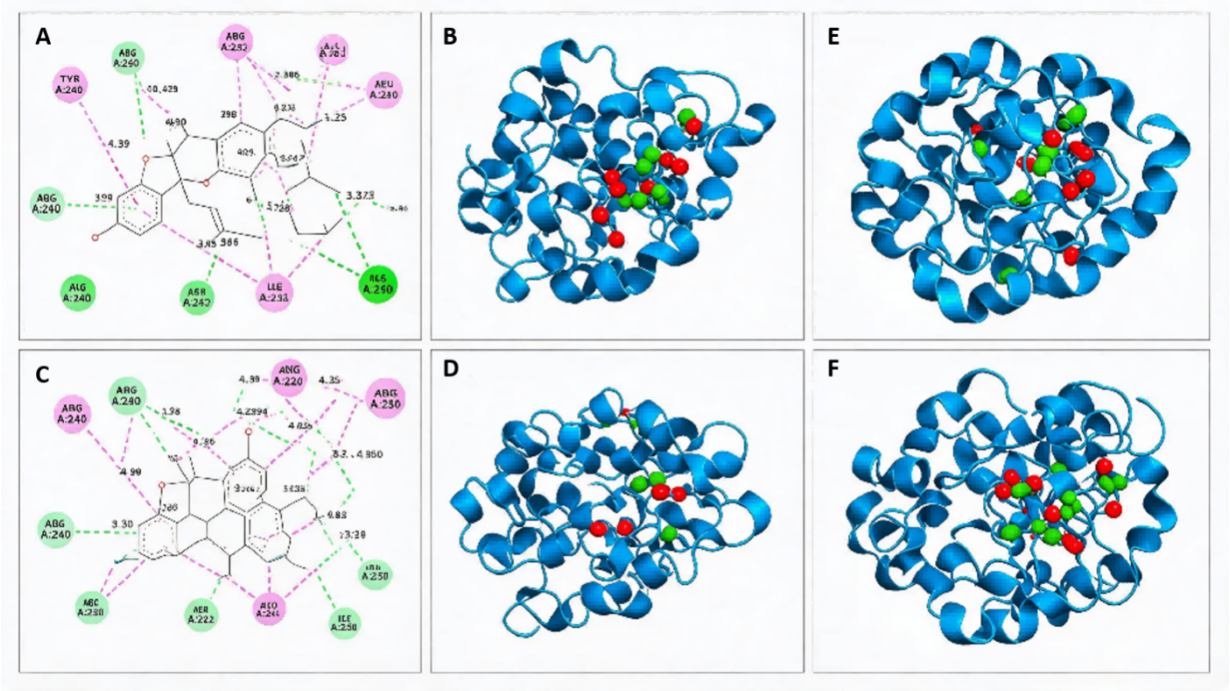


Figure 6. Two-dimensional and three-dimensional ligand–receptor interaction diagrams for sanggenol-type flavonoids docked against the peroxisome proliferator-activated receptor gamma protein via AutoDock Vina 1.1.2. Two-dimensional interaction diagrams of (A) sanggenol L and (C) sanggenol I. Corresponding three-dimensional binding conformation visualizations for (B) sanggenol L, (D) sanggenol I, and (E, F) sanggenon M. All docking outputs represent computational simulation results.

The identified bioactive ingredients are mainly prenol lipids (from Aconiti lateralis radix praeparata and Ginseng radix et rhizoma), flavonoids (from Mori cortex), and anthracenes (from Rhei radix et rhizoma). Published literature has documented their antiinflammatory, antioxidant, antifibrotic, and cardioprotective pharmacological activities.[15-19] These compounds may act synergistically to improve myocardial contractile performance, inhibit pathological ventricular remodeling, and sustain intracellular calcium homeostasis in cardiomyocytes.

Kyoto Encyclopedia of Genes and Genomes enrichment results showed that SFQXP predominantly modulates neuroactive ligand–receptor interactions and the cGMPPKG, cAMP, and calcium signaling pathways. The cGMPPKG signaling pathway plays a pivotal protective role in suppressing myocardial hypertrophy and interstitial fibrosis. cAMP and calcium signaling participate in myocardial excitation–contraction coupling; excessive intracellular calcium overload drives HF progression. Based on our computational enrichment results, we hypothesize that SFQXPderived compounds might mitigate HFrelated pathological changes by regulating calcium homeostasis and ventricular remodeling; this conjecture needs experimental verification in HF animal models.

Molecular docking simulation predicted favorable binding interactions between sanggenol A and PPARG. PPARG functions as a nuclear receptor that regulates inflammatory responses, lipid metabolism, and myocardial fibrosis. PPARG activation may be a critical molecular mechanism by which SFQXP slows pathological deterioration in HF. Docking results for three additional sanggenoltype flavonoids further support this compound–target interaction (Table 3, Figure 6). Nevertheless, such docking observations stem exclusively from *in silico* simulation. Direct biochemical or cellular assays are required to confirm physical binding and functional modulation between sanggenol-type flavonoids and PPARG.

Several limitations of this work should be acknowledged. In addition, the disease–target database source and threshold settings (e.g., GeneCards relevance score > 5) may introduce analytical bias, and changing filtering thresholds can alter individual core target lists and enrichment outputs. No formal sensitivity analysis across multiple cutoffs was performed in the current study. First, isomeric compounds could not be comprehensively

differentiated by the current mass spectrometry workflow. Second, network pharmacology outputs remain computational predictions requiring further experimental validation. In addition, the molecular docking simulation adopted an AlphaFold-predicted PPARG structure with full-protein semi-blind docking; crystallographically solved protein structures with defined binding pockets are preferred for higher-confidence docking assessment. Third, only rat serum samples were analyzed in this investigation. In the rat medicatedserum study, serum samples from multiple animals within the same group and time point were pooled before instrumental measurement. This pooling strategy prevents estimation of interanimal biological variance and prohibits formal sample size power calculation for individualrat observations. Followup research should focus on cellular and animal model experiments to verify the functional roles of cGMPPKG and cAMPcalcium signaling cascades.

Caution should be exercised when extrapolating these findings toward human clinical settings. Serum chemical profiling was conducted using healthy rats. Drug absorption, metabolic transformation, and circulating compound concentrations may change substantially under HF pathological conditions. All target and pathwayrelated hypotheses were derived purely from computational prediction rather than experimental evidence, and interspecies pharmacokinetic differences exist between rats and humans. Before any therapeutic conclusions or clinical translation can be reasonably considered, a series of sequential validating experiments are required, including *in vitro* cardiomyocyte functional assays, HF animal model studies with cardiac functional readouts such as echocardiography and myocardial injury biomarkers, targetengagement verification, and subsequent clinical pharmacology investigations.

Collectively, our computational hypotheses suggest that SFQXPderived constituents may act through multiple chemical ingredients, functional targets, and signaling pathways, principally by maintaining calcium homeostasis, restraining ventricular remodeling, and modulating neuroendocrine activities. Our findings generate scientific hypotheses and lay preliminary groundwork for follow-up mechanistic verification and clinical research on SFQXP.[15-17]

5. Conclusion

This UHPLC-Q-Orbitrap HRMS and network pharmacology study profiles SFQXP and generates computational hypotheses about HFassociated targets and signaling cascades. No functional pharmacological validation was performed. Further experiments using HF animal models are needed to test these predicted targets and pathways.

Acknowledgments

None.

Funding

This work was supported by the Key Scientific Research Project in Traditional Chinese Medicine of Tianjin (Grant No. 2024015) and the Traditional Chinese Medicine and Integrated ChineseWesternMedicine Scientific Research Project of Tianjin Health Commission (Grant No.2025083).

Conflicts of interest

The authors declare that there are no conflicts of interest.

Author contributions

Conceptualization: Haiyun Zhu
Formal analysis: Yingdong Wu
Investigation: Yingdong Wu
Methodology: Haiyun Zhu
Writing – original draft: Haiyun Zhu
Writing – review & editing: Haiyun Zhu

Ethics approval and consent to participate

All animalexperiment procedures obtained formal approval from the Institutional Animal Care and Use Committee (approval No.: IACUCGENINK20250160). All experimental manipulations complied with the Guide for the Care and Use of Laboratory Animals.

Consent for publication

Not applicable.

Availability of data

The raw UHPLCQOrbitrap HRMS datasets, processed analytical data supporting the findings of this study, and datasets generated and/or analyzed during the current study are available from the corresponding author upon reasonable request.

AI tools statement

Portions of text composition, language refinement, and figure caption preparation of this manuscript were performed with artificial intelligence assistance (Doubao, ByteDance). All experimental datasets, bioinformatic analysis interpretation, scientific inference, conclusions, and final manuscript approval are the work of the authors. All authors take complete accountability for all information presented in this article.

References

1. Chinese Society of Cardiology, Chinese Medical Association; Chinese College of Cardiovascular Physician; Chinese Heart Failure Association of Chinese Medical Doctor Association; Editorial Board of Chinese Journal of Cardiology. Zhongguo xinli shuaijie zhenduan he zhiliao zhinan 2024 [2024 Chinese guidelines for the diagnosis and treatment of heart failure]. *Chin J Cardiol*. 2024;52(3):235-275. [In Chinese].

   doi: 10.3760/cma.j.cn112148-20231101-00405

2. Aşkin L, Tanriverdi O. The benefits of sacubitril-valsartan in low ejection fraction heart failure. *Abant Med J*. 2022;11(3):336-337.

   doi: 10.47493/abantmedj.1182158

3. Sun Y. Ma Lianzhen yi Shenfu Qiangxin Wan bianzhi manxing xinshuai jingyan [Professor Ma Lianzhen's experience in differentiating and treating chronic heart failure with Shenfu Qiangxin Pill]. *Chin J Basic Med Tradit Chin Med*. 2012;18(7):745-746. [In Chinese].

   doi: 10.19945/j.cnki.issn.1006-3250.2012.07.023

4. Yuan H, Zhang DW, Ma XH. Shenfu Qiangxin Wan zhiliao xinli shuaijie youxiaoxing ji anquanxing de Meta fenxi [Efficacy and safety of Shenfu Qiangxin Pill for heart failure: a meta-analysis]. *Chin J Integr Med Cardio Cerebrovasc Dis*. 2021;19(16):2693-2700. [In Chinese].

   doi: 10.12102/j.issn.1672-1349.2021.16.003

5. Wei YQ, Liu Y, Meng ZR, *et al*. Shenfu Qiangxin Wan lianhe changgui liaofa zhiliao manxing xinli shuaijie de Meta fenxi [Efficacy and safety of Shenfu Qiangxin Pill combined with conventional therapy for chronic heart failure: a meta-analysis]. *China Pharmacy*. 2021;32(6):736-742. [In Chinese].

   doi: 10.6039/j.issn.1001-0408.2021.06.16

6. Ma ZY. Shenfu Qiangxin Wan duibi leimipuli zhiliao manxing chongxuexing xinlishuaijie de linchuang liaoxiao [Clinical efficacy of Shenfu Qiangxin Pill vs ramipril in chronic congestive heart failure]. *Pract Clin J Integr Tradit West Med*. 2023;23(14):41-43. [In Chinese]

7. Zhang X, Jin Q, Zhuo XM. Shakubaqu xieshatan lianhe Shenfu Qiangxin Wan zhiliao manxing xinli shuaijie de linchuang liaoxiao [Clinical efficacy of sacubitril valsartan combined with Shenfu Qiangxin Pill in chronic heart failure]. *Contemp Med*. 2021;27(29):127-128. [In Chinese]

8. Xiong S, Zhao YL, Han S. Shenfu Qiangxin Wan fuzhi manxing xinli shuaijie linchuang guancha [Clinical observation of Shenfu Qiangxin Pill in adjuvant treatment of chronic heart failure]. *J Pract Tradit Chin Med*. 2024;40(7):1299-1301. [In Chinese]

9. Yang Y, Yao CL, Guo DA. Insight into chemical basis of traditional Chinese medicine based on liquid chromatography mass spectrometry. *Acta Pharm Sin B*. 2021;11(6):1469-1492.

   doi: 10.1016/j.apsb.2021.02.017

10. Xia Q, Liu M, Li H, *et al*. Network pharmacology strategy to investigate the pharmacological mechanism of HuangQiXiXin decoction on cough variant asthma. *Evid Based Complement Alternat Med*. 2020;2020(1):3829092.

    doi: 10.1155/2020/3829092

11. Kanehisa M, Goto S. KEGG: Kyoto Encyclopedia of Genes and Genomes. *Nucleic Acids Res*. 2000;28(1):27-30.

    doi: 10.1093/nar/28.1.27

12. Trott O, Olson AJ. AutoDock Vina: improving the speed and accuracy of docking with a new scoring function, efficient optimization, and multithreading. *J Comput Chem*. 2010;31(2):455-461.

    doi: 10.1002/jcc.21334

13. Hsin KY, Ghosh S, Kitano H. Combining machine learning systems and multiple docking simulation packages to improve docking prediction reliability for network pharmacology. *PLoS One*. 2013;8(12):e83922.

    doi: 10.1371/journal.pone.0083922

14. Xu H, Wang W, Li X, *et al*. Botany, traditional use, phytochemistry, pharmacology and clinical applications of rhubarb (*Rhei Radix et Rhizome*): a systematic review. *Am J Chin Med*. 2024;52(7):1925-1967.

    doi: 10.1142/S0192415X24500757

15. Wu Z, Qian J, Feng C, *et al*. A review of *Aconiti Lateralis Radix Praeparata* (Fuzi) for kidney disease: phytochemistry, toxicology, herbal processing, and pharmacology. *Front Pharmacol*. 2024;15:1427333.

    doi: 10.3389/fphar.2024.1427333

16. Li Y, Wang H, Zhang Y. Exploring the therapeutic and antitumor properties of morusin: a review of recent advances. *Front Mol Biosci*. 2023;10:1168298.

    doi: 10.3389/fmolb.2023.1168298

17. Evans LW, Ferguson BS, McKinsey TA. Emodin and emodin-rich rhubarb inhibits histone deacetylase (HDAC) activity and cardiac myocyte hypertrophy. *J Nutr Biochem*. 2020;79:108339.

    doi: 10.1016/j.jnutbio.2019.108339

18. Wang Z, Li Y, Zhang L. Unlocking ginsenosides' therapeutic power with polymer-based delivery systems: current applications and future perspectives. *Front Pharmacol*. 2025;16:1629803.

    doi: 10.3389/fphar.2025.1629803

19. Li Y, Jiang JG. Health functions and structure-activity relationships of natural anthraquinones from plants. *Food Funct*. 2018;9(12):6063-6080.

    doi: 10.1039/C8FO01569D